Advanced Dynamic Motorbike Analysis and Driver Simulation

Thorsten Breuer

Dipl.-Ing. Alfred Pruckner

Institut für Kraftfahrwesen Aachen

RWTH Aachen

Steinbachstr. 10

52074 Aachen - Germany

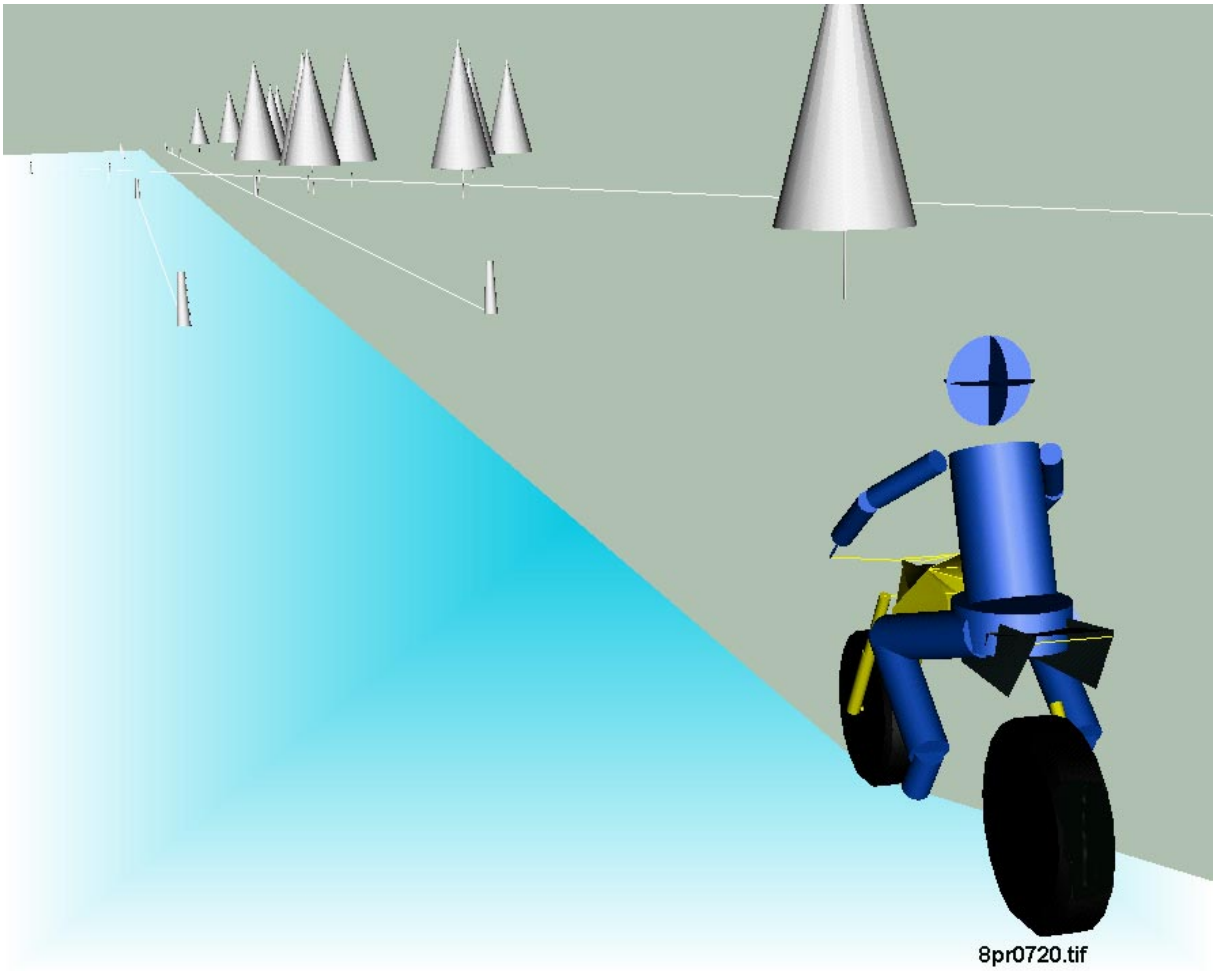

1 Abstract

Motorbike sales have been steadily rising within the last years due to the increasing traffic density in urban centres and for recreational activities as well. Consequently, the requirements for high speed stability and maximum handling performance are continuously increasing although they are resulting in opposing chassis layout demands. A major criterion for a motorbike's high speed stability is the so-called weave mode phenomenon which should be suppressed under all circumstances as it may provoke extremely dangerous driving situations. The weave mode is an eigenvalue vibration with decreasing damping coefficient at increasing vehicle velocity.

Another important field of investigation is the development of modern motorbike brake systems including ABS (Antilock Brake System) and a combined operation of front and rear wheel brakes as in normal motorcars.

All these developments are supposed to enhance the active safety of motorbikes; however, development tools for motorbike vehicle dynamics are hard to find and mostly only linear simulation models with only few degrees of freedom are employed. Moreover, tyre behaviour is in most cases still assumed to be linear and compliance effects in the suspensions are normally not considered.

In this contribution the possibilities of a motorbike vehicle dynamics simulation employing the multibody simulation tool ADAMS will be displayed. Particularly the weave mode characteristics of a motorbike model will be compared to a simplified analytical model and different influences of model improvements on the results will be shown.

Therefore various driving manoeuvres as cornering and double lane change with a specially designed driver control algorithm have been simulated and the results will be presented. Furthermore, a new brake system developed at the *Institut für Kraftfahrwesen Aachen* which combines ABS and a combined operation of the wheel brakes will be analysed using the simulation model as well. The results of these braking manoeuvre simulations will be compared to data from real driving tests.

2 Wave Mode Calculation

2.1 Theory

The dynamic motorbike behaviour can be estimated by the use of a simple model shown in Fig. 2-1. This model consists of 4 parts. The main body with the driver fixed on it, the steering system and both wheels. The model is defined as 4 degrees of freedom model with the following state space variables: lateral movement (y-axis), steering wheel input (λ), yaw movement about the z-axis (γ) and roll movement about x-axis (ρ).

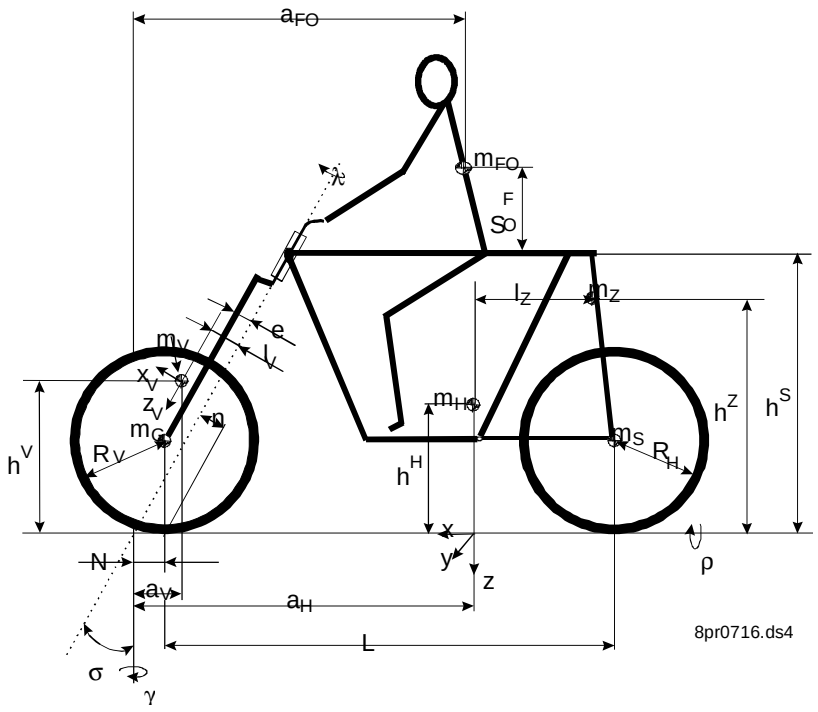

Fig. 2-1: Simplified Motorbike-Model

This simplified 4 mass model with 4 degrees of freedom causes the following 4 differential equations of motion [KOC80]:

Force equation in y-axis Eq: 2-1

$$(m_V + m_H + m_S + m_G + m_{FO}) \cdot \ddot{v} + (m_V \cdot h_V + m_H \cdot h_H + m_S \cdot R_H + m_G \cdot R_V + m_{FO} \cdot (h_S + s_{FO})) \cdot \dot{\omega} + (m_V \cdot (a_H - a_V) + m_G \cdot (a_H - N) - m_S \cdot (L + N - a_H)) \cdot \dot{\psi} + (m_V \cdot l_V + m_G \cdot e) \cdot \ddot{\lambda} + (m_V + m_H + m_S + m_G + m_{FO}) \cdot U \cdot \dot{\gamma} - F_{SV} - F_{SH} = 0$$

Torque equation about z-axis Eq: 2-2

$$(m_V \cdot (a_H - a_V) + m_G \cdot (a_H - N) - m_S \cdot (L + N - a_H) + m_{FO} \cdot (a_H - a_{FO})) \cdot \ddot{v} + (m_V \cdot h_V \cdot (a_H - a_V) + m_G \cdot R_V \cdot (a_H - N) - m_S \cdot R_H \cdot (L + N - a_H) - \theta_{Hxz} + (I_{Vz} - I_{Vx}) \cdot \sin(\sigma) \cdot \cos(\sigma) + (I_{Gz} - I_{Gx}) \cdot \sin(\sigma) \cdot \cos(\sigma) + m_{FO} \cdot (h_S + s_{FO}) \cdot (a_H - a_{FO})) \cdot \dot{\omega} + (m_V \cdot (a_H - a_V)^2 + m_G \cdot (a_H - N)^2 + m_S \cdot (L + N - a_H)^2 + \theta_{Hz} + \theta_{Sz} + I_{Vx} \cdot \sin(\sigma)^2 + I_{Gx} \cdot \sin(\sigma)^2 + I_{Vz} \cdot \cos(\sigma)^2 + I_{Gz} \cdot \cos(\sigma)^2) \cdot \ddot{\psi} + (m_V \cdot l_V \cdot (a_H - a_V) + I_{Vz} \cdot \cos(\sigma) + m_G \cdot e \cdot (a_H - N) + I_{Gz} \cdot \cos(\sigma)) \cdot \ddot{\lambda} + (I_{Vy} / R_V + I_{Hy} / R_H + I_{Ey} \cdot i) \cdot U \cdot \dot{\omega} + (m_V \cdot (a_H - a_V) + m_G \cdot (a_H - N) - m_S \cdot (L + N - a_H) + m_{FO} \cdot (a_H - a_{FO})) \cdot U \cdot \dot{\gamma} + (I_{Vy} / R_V \cdot \sin(\sigma)) \cdot U \cdot \dot{\lambda} - (a_H - N) \cdot F_{SV} + (L + N + a_H) \cdot F_{SH} + M_{ZV} + M_{ZH} = 0$$

Torque equation about x-axis Eq: 2-3

$$\begin{aligned}
&\left(m_V \cdot h_V + m_H \cdot h_H + m_S \cdot R_H + m_G \cdot R_V + m_{FO} \cdot (h_S + s_{FO})\right) \cdot \ddot{\vartheta} + \\
&\left(m_V \cdot h_V^2 + m_H \cdot h_H^2 + m_G \cdot R_V^2 + m_S \cdot R_H^2 + \theta_{Hx} + \theta_{Sx} + I_{Vx} \cdot \cos(\sigma)^2 + I_{Vz} \cdot \sin(\sigma)^2 + \right. \\
&\left. I_{Gx} \cdot \cos(\sigma)^2 + I_{Gz} \cdot \sin(\sigma)^2 + \theta_\chi + m_{FO} \cdot (h_S + s_{FO})^2\right) \cdot \ddot{\rho} + \\
&\left(m_V \cdot h_v \cdot (a_H - a_V) + m_G \cdot R_V \cdot (a_H - N) - m_S \cdot R_H \cdot (L + N - a_H) - \theta_{Hxz} + \right. \\
&\left. (I_{Vz} - I_{Vx}) \cdot \sin(\sigma) \cdot \cos(\sigma) + (I_{Gz} - I_{Gx}) \cdot \sin(\sigma) \cdot \cos(\sigma)\right) \cdot \ddot{\varphi} + \\
&\left(m_V \cdot l_V \cdot h_V + I_{Vz} \cdot \sin(\sigma) + m_G \cdot e \cdot R_V + I_{Gz} \cdot \sin(\sigma)\right) \cdot \ddot{\chi} + \\
&(m_V \cdot h_V + m_H \cdot h_H + m_S \cdot R_H + m_G \cdot R_V + m_{FO} \cdot (h_S + s_{FO}) + I_{Vy} / R_V + I_{Hy} / R_H + I_{Ey} \cdot i) \cdot U \cdot \dot{\varphi} + \\
&\left(I_{Vy} / R_V \cdot \cos(\sigma)\right) \cdot U \cdot \dot{\chi} - \left(m_V \cdot h_V + m_H \cdot h_H + m_S \cdot R_H + m_G \cdot R_V - m_{FO} \cdot (h_S + s_{FO})\right) \cdot g \cdot \rho + \\
&(F_N \cdot n - m_V \cdot l_V \cdot g - m_G \cdot e \cdot g) \cdot \lambda + M_{Vx} + M_{Hx} = 0
\end{aligned}$$

Torque equation about steering-axis Eq: 2-4

$$\begin{aligned}
&(m_V \cdot l_V + m_G \cdot e) \cdot \ddot{\vartheta} + \left(m_V \cdot l_V \cdot h_V + I_{Vz} \cdot \sin(\sigma) + m_G \cdot e \cdot R_V + I_{Gz} \cdot \sin(\sigma)\right) \cdot \ddot{\rho} + \\
&\left(m_V \cdot l_V \cdot (a_H - a_V) + I_{Vz} \cdot \cos(\sigma) + m_G \cdot e \cdot (a_N - N) + I_{Gz} \cdot \cos(\sigma) + \theta_\chi\right) \cdot \ddot{\varphi} + \\
&\left(I_{Vz} + m_V \cdot l_V^2 + I_{Gz} + m_G \cdot e^2 + \theta_{ML}\right) \cdot \ddot{\chi} - I_{Vy} / R_V \cdot \cos(\sigma) \cdot U \cdot \dot{\rho} + \\
&\left(m_V \cdot l_V + m_G \cdot e + I_{Vy} / R_V \cdot \sin(\sigma)\right) \cdot U \cdot \dot{\varphi} + (r_L + r_{ML}) \cdot \dot{\chi} + \left(F_N \cdot n - m_V \cdot l_V \cdot g - m_G \cdot e \cdot g\right) \cdot \rho + \\
&\left((F_N \cdot n - m_V \cdot l_V \cdot g - m_G \cdot e \cdot g) \cdot \sin(\sigma) + k_{ML}\right) \cdot \lambda + \\
&n \cdot F_{SV} + M_{ZV} \cdot \cos(\sigma) + M_{XV} \cdot \sin(\sigma) = 0
\end{aligned}$$

In these complex equations of motions with integrated gyroscope physics both tyre forces and torques has to be modelled as functions of the state space variables. The calculated side slip and roll angles on the front and rear wheel can be found in the following equations:

$$\alpha_V = \lambda \cdot \cos\sigma - \frac{\dot{\vartheta} + (a_H - N) \cdot \dot{\varphi} - n \cdot \dot{\chi}}{U} \qquad \text{Eq: 2-5}$$

$$\alpha_H = \frac{(L + N - a_H) \cdot \dot{\varphi} - \dot{\vartheta}}{U} \qquad \text{Eq: 2-6}$$

$$\rho_V = \rho + \lambda \cdot \sin\sigma \qquad \rho_H = \rho \qquad \text{Eq: 2-7}$$

At least this formulas can be changed over in the following matrices:

$$\underline{M} \cdot \ddot{\vec{y}} + \underline{K} \cdot \dot{\vec{y}} + \underline{C} \cdot \vec{y} = 0 \qquad \text{Eq: 2-8}$$

$$\underline{M} = \begin{bmatrix} M_{1,1} & \cdots & M_{1,8} \\ \vdots & & \vdots \\ M_{8,1} & \cdots & M_{8,8} \end{bmatrix} \qquad \underline{K} = \begin{bmatrix} K_{1,1} & \cdots & K_{1,8} \\ \vdots & & \vdots \\ K_{8,1} & \cdots & K_{8,8} \end{bmatrix} \qquad \underline{C} = \begin{bmatrix} C_{1,1} & \cdots & C_{1,8} \\ \vdots & & \vdots \\ C_{8,1} & \cdots & C_{8,8} \end{bmatrix}$$

The eigenvalue analyses of Eq. 2-9 delivers different complex eigenvalues. The real term indicates the damping ratio, the imaginary term presents the damped frequency. So called rigid body modes and over critical damped eigenvalues have no imaginary term, the sign of the real term in each eigenvalue informs about the stability of the eigenvalue. Negative real terms mean stable eigenvalues, real terms at zero mean permanent but limited oscillation and positive real terms inform about non stable system behaviour.

Eq. 2-8 has been built up in the regulation software MATLAB [MAT96], one of the estimated eigenvalues can be recognized as the so called wave mode. The following Fig. 2-2 shows the eigenvalues of this estimation depending on the motorbike velocity (Model 1) [JAN98].

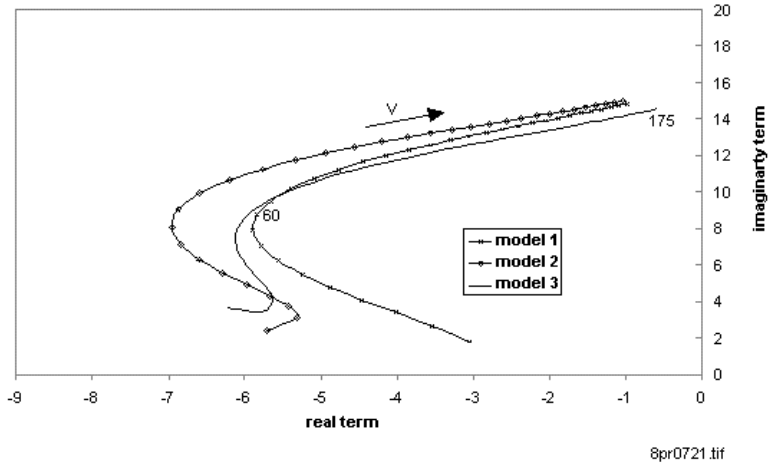

Fig. 2-2: Wave mode, comparison of different tyre models

To recognise the influence of different tyre models, the lateral tyre forces are modelled as first order differential equations what increases the number of state values up to 6 (Model 2). Model 3 shows the improvement in case of additional first order aligning torque calculation (all in all 8 state space values).

All three tyre models present increasing frequencies for higher velocities. Dangerous, practical high speed tests show wave mode frequencies up to 3 Hz near the non-stable region [BAY86]. These tests show decreasing system damping too for increasing speeds. Increasing negative real terms shown in Fig. 2-2 cannot be found in practical tests. Since the improvement of the tyre model reduces this phenomenon, the reason for this can be found in the simplification of the mathematical model.

2.2 ADAMS Eigenvalue estimation

To see the possibilities in the ADAMS Eigenvalue estimation, a simple ADAMS motorbike with to parts and two tyre statements has been modelled (Fig. 2-1). Different tyre models with simple linear tyre characteristics have been used as well as a more complex UA-tyre model.

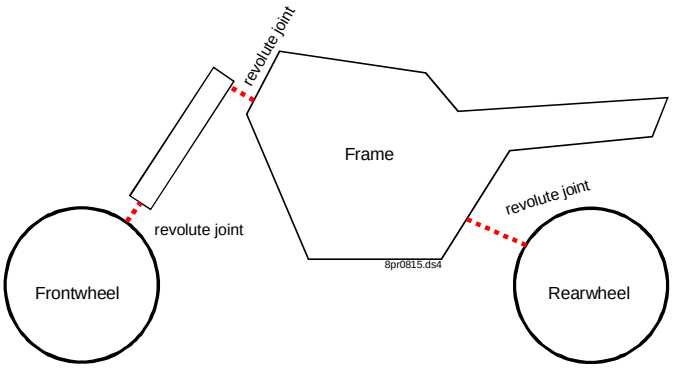

Fig. 2-1: Simple ADAMS motorbike model

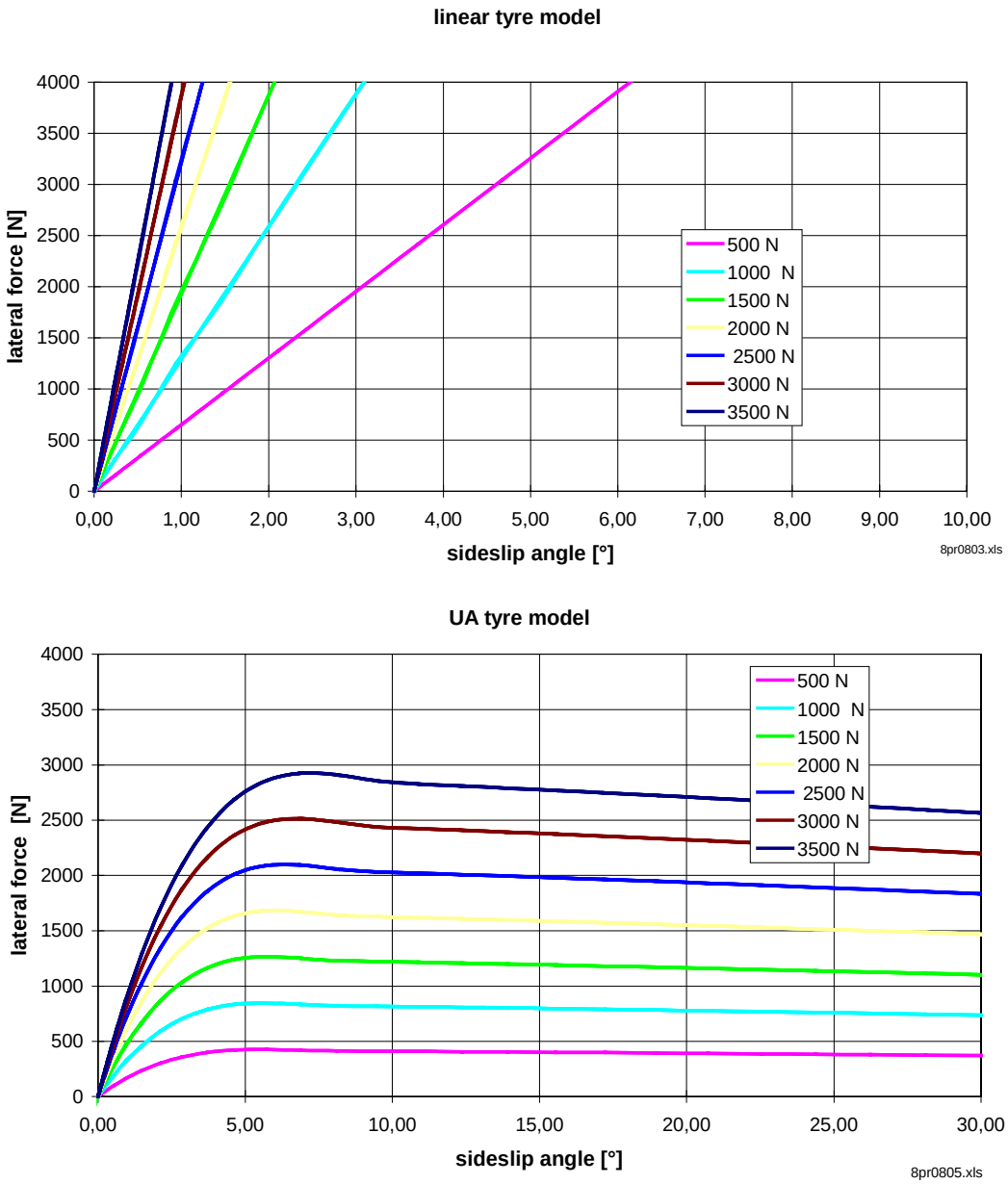

Fig. 2-2: Simple and complex lateral tyre force model due to side slip angle

Fig. 2-2 shows the lateral tyre forces with respect to the side slip angle in case of the simple linear tyre model and the complex University of Arizona (UA) tyre model. The lateral tyre force due to camber angle to both tyre models can be seen in the following Fig. 2-3.

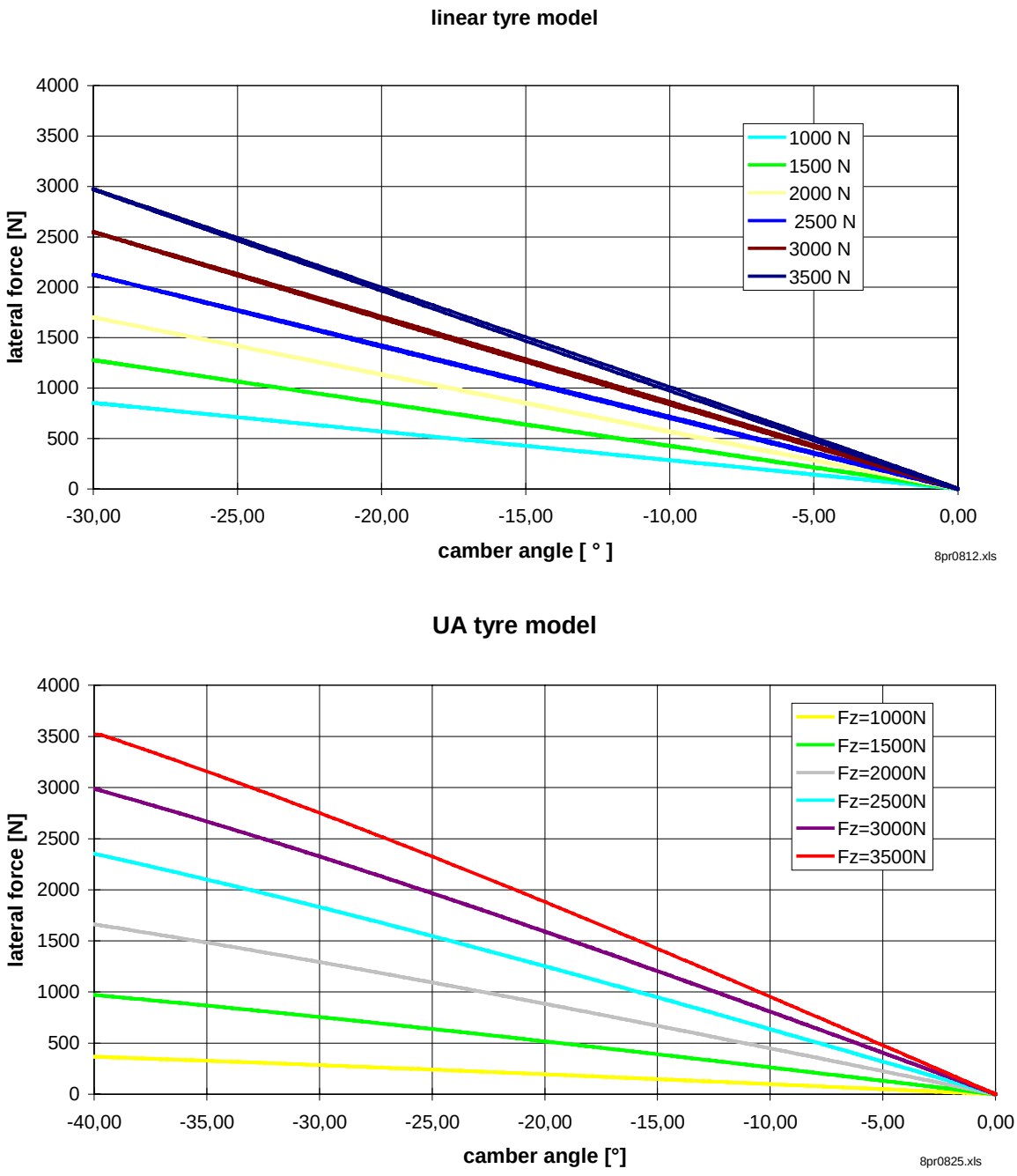

Fig. 2-3: Simple and complex lateral tyre force model due to camber angle

The lateral tyre force due to both, side slip and camber angle at the same time, is shown in the next Fig. 2-4. Unlike the linear tyre model the mutual influence of side slip and camber angle will be taken into consideration by the UA-tyre model.

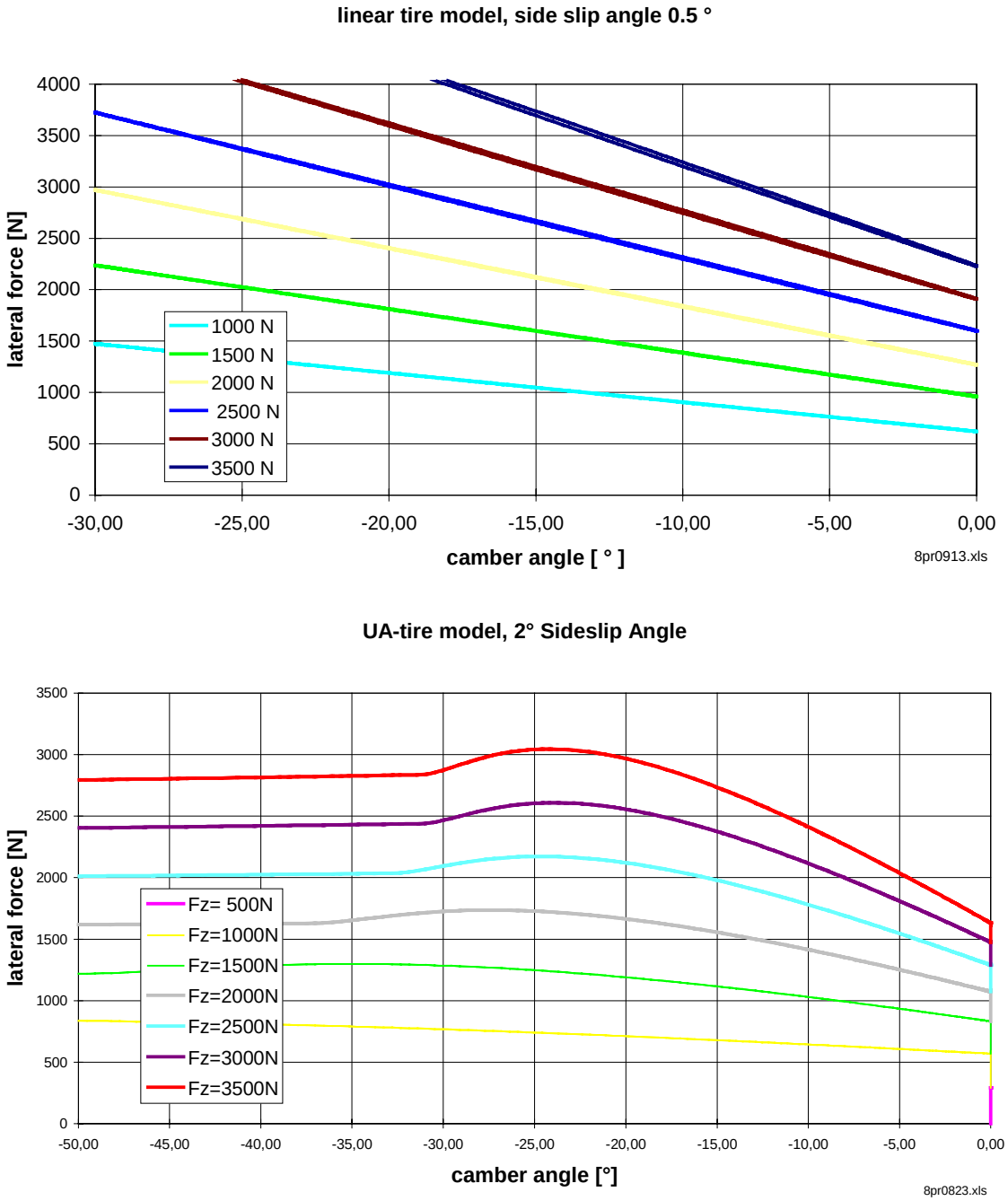

Fig. 2-4: Simple and complex lateral tyre force model due to camber angle with additional constant side slip angle

The linear eigenvalue estimation in ADAMS has been done after a certain dynamic system calculation. This has to be done to be sure that the motorbike is in a quasi static state at that moment. Fig. 2-5 shows the results of the eigenvalue analysis in ADAMS. However, even if the bike model is similar to the mathematical model in chapter 2.1, the values are too small. Only the trend to growing real and imaginary terms up to positive real terms (loss of stability) can be foreseen.

The reason for this problem may be found in the ADAMS integrated tyre model, experimental tests to show the actual tyre mass and mass moment of inertia brought wrong data during the estimation.

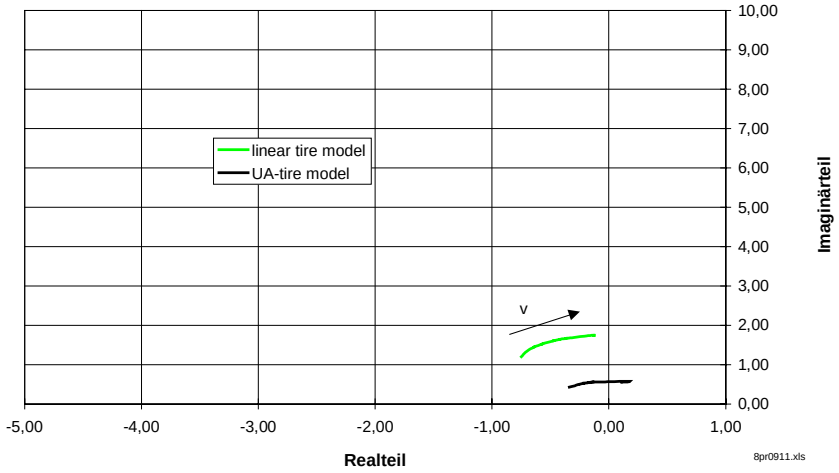

Fig. 2-5: Eigenvalues estimated from ADAMS with integrated ADAMS tyre model

To bypass this problem a totally different bike model has been analysed. Fig. 2-6 shows the rigid body constellation of this ADAMS model without integrated ADAMS tyre model. Both wheels are modelled as simple *parts* and connected to the main body respectively steering system. The *rotational motion* is linked to the motorbike velocity in a certain way. The steering system is connected to the main body by a *revolute joint*, both, steering system and main body are connected to the ground by *inplane joints*. These '*joint primitives*' constrains one degree of freedom. All in all the system shown in Fig. 2-6 contents 5 degrees of freedom.

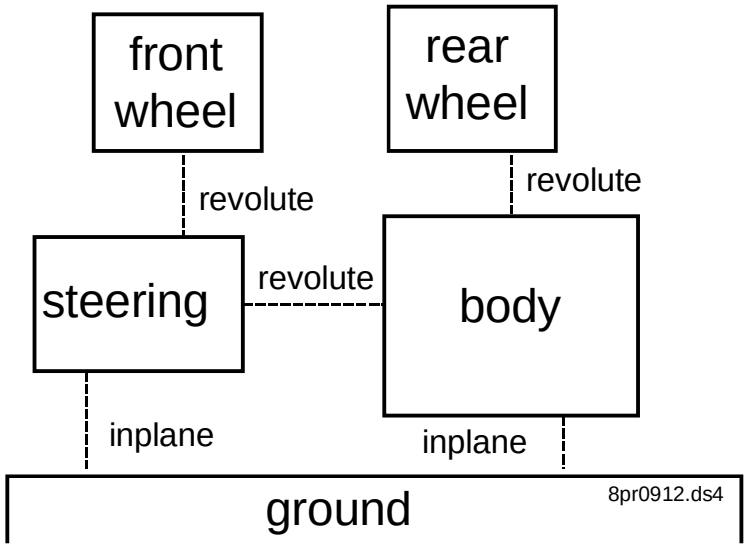

Fig. 2-6: ADAMS bike model without integrated tyre model

The contact forces between bike and environment are modelled as so called *gforces* in lateral direction as well as aligning torque around the z-axis and overturning moment about the roll axis. The forces are estimated as linear depending on side slip angle and roll angle, the static force and torque values are extended by transfer functions to take the dynamic tyre behaviour into consideration.

At least this model has been simulated dynamically for one second to get quasi static behaviour followed by the eigenvalue analysis. The results of these tests can be seen in the following figure.

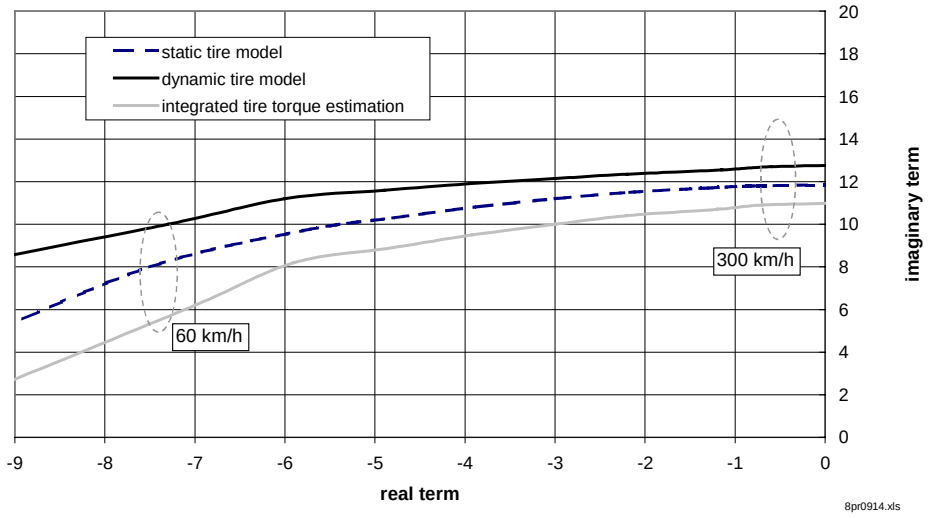

Fig. 2-7: Wave mode calculation with simple tyre model

Fig. 2-7 shows that especially for velocities higher than 60 km/h the results of the ADAMS eigenvalue estimation matches the MATLAB results (Fig. 2-2) as well as practical driving tests [BAY86]. Critical driving situations can be found in high speed regions near 300 km/h. Simulations with a different bike model (smaller wheel base, less mass and mass moment of inertia) show that the critical wave mode speed is reduced to 230 km/h.

3 Longitudinal dynamic simulation

The longitudinal motorbike simulation shows advantages by the use of combined brake systems. The *Institut für Kraftfahrwesen Aachen* owns a multifunctional test bike with different useable brake systems. The combined system with controlled rear wheel pressure just in case of front brake lever use has been completed by two ABS Modules on both wheels (Fig. 3-1).

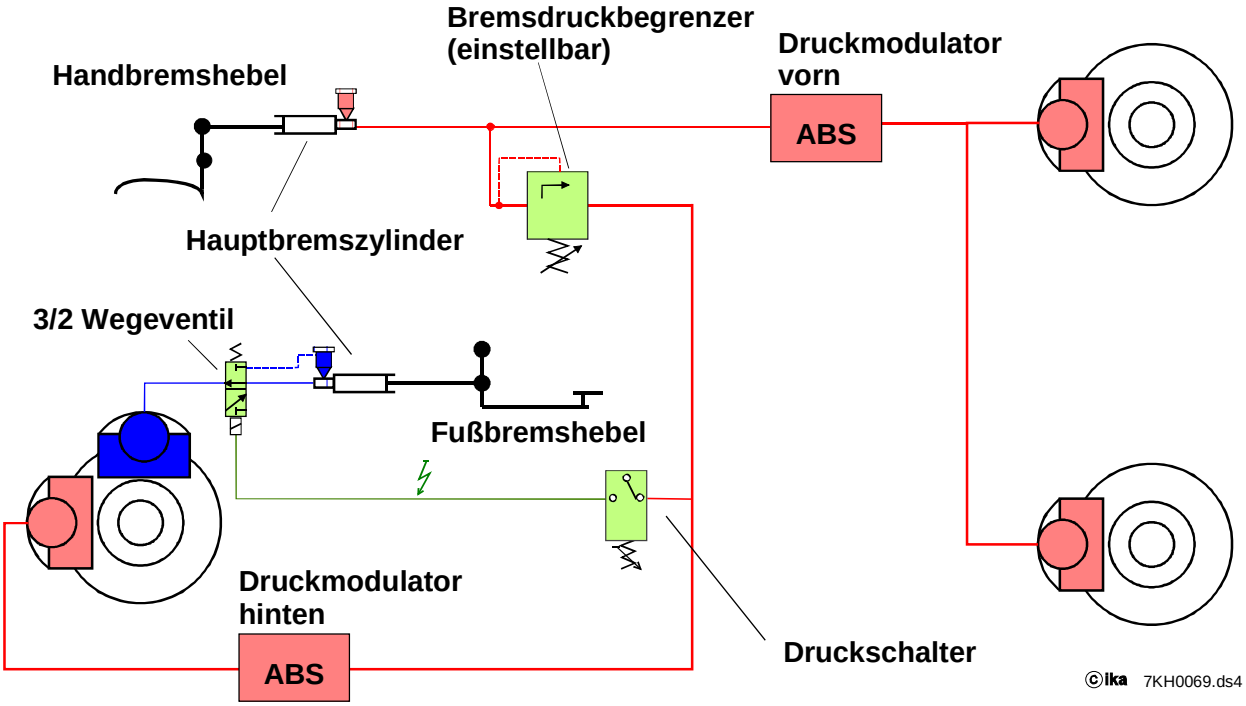

Fig. 3-1: ika combined brake system

To figure out the advantages of the combined brake system, three different full braking manoeuvres at 80 km/h on wet road conditions have been done: the first manoeuvre with full locked rear wheel (without ABS), the second manoeuvre with front ABS intervention and the third one with combined ABS intervention on both wheels. Tab. 3-1 shows the expected results to this manoeuvres.

System	Brake distance [m]
$R_{\text{without ABS}}$	85
F_{ABS}	38
F/R_{ABS}	32

Tab. 3-1: Braking distance on wet test track

To show advantages of combined brake systems four braking manoeuvres with two different bike models have been simulated. A simple 9 degrees of freedom model without any suspension (Fig. 2-1) and an improved model with two additional degrees of freedom and integrated spring damper (Fig. 3-2).

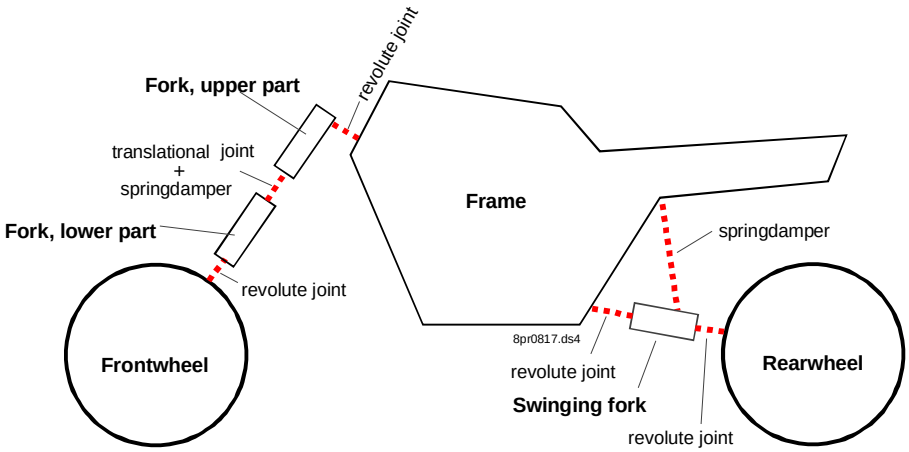

Fig. 3-2: Improved ADAMS motorbike model

Both models, the simple and the improved one use the same tyre model, which longitudinal tyre force characteristic can be seen in Fig. 3-3.

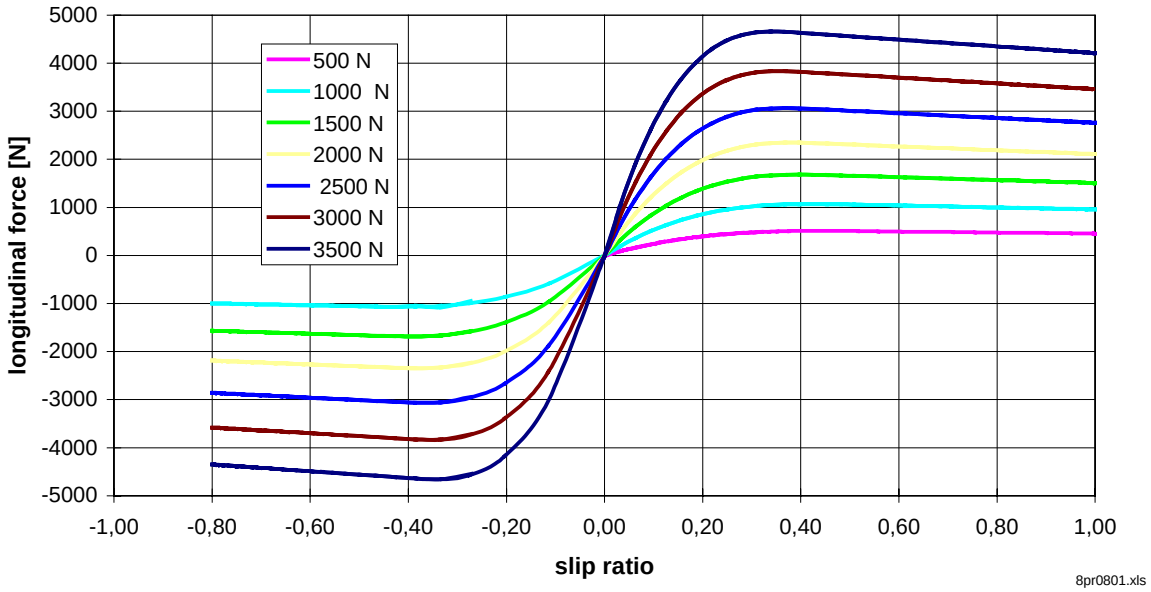

Fig. 3-3: Longitudinal tyre force characteristic, UA tyre model

The next Fig. 3-4 shows the braking distance for these simulations in both cases, with and without suspension [BRE98]. Both models deliver the same distance except of the rear wheel ABS braking manoeuvre, where the suspended bike profits from higher rear wheel loads, which follows from the rear suspension kinematic.

The front wheel braking intervention shortens the braking distance in any case, additional rear wheel braking intervention reduces the brake distance again. In comparison to the test

track results (Tab. 3-1), the use of both ABS systems match the real distance (32m) well. The brake distance with only front wheel intervention delivers higher values in case of the simulation (50m), which follows from the fixed driver on the ADAMS bike model. Different to the combined ABS intervention, the influence of the driver cannot be disregarded in that case. The smaller brake distance with locked rear wheel in the simulation can be found in certain brake interventions on the test track which the driver used to stabilize the bike.

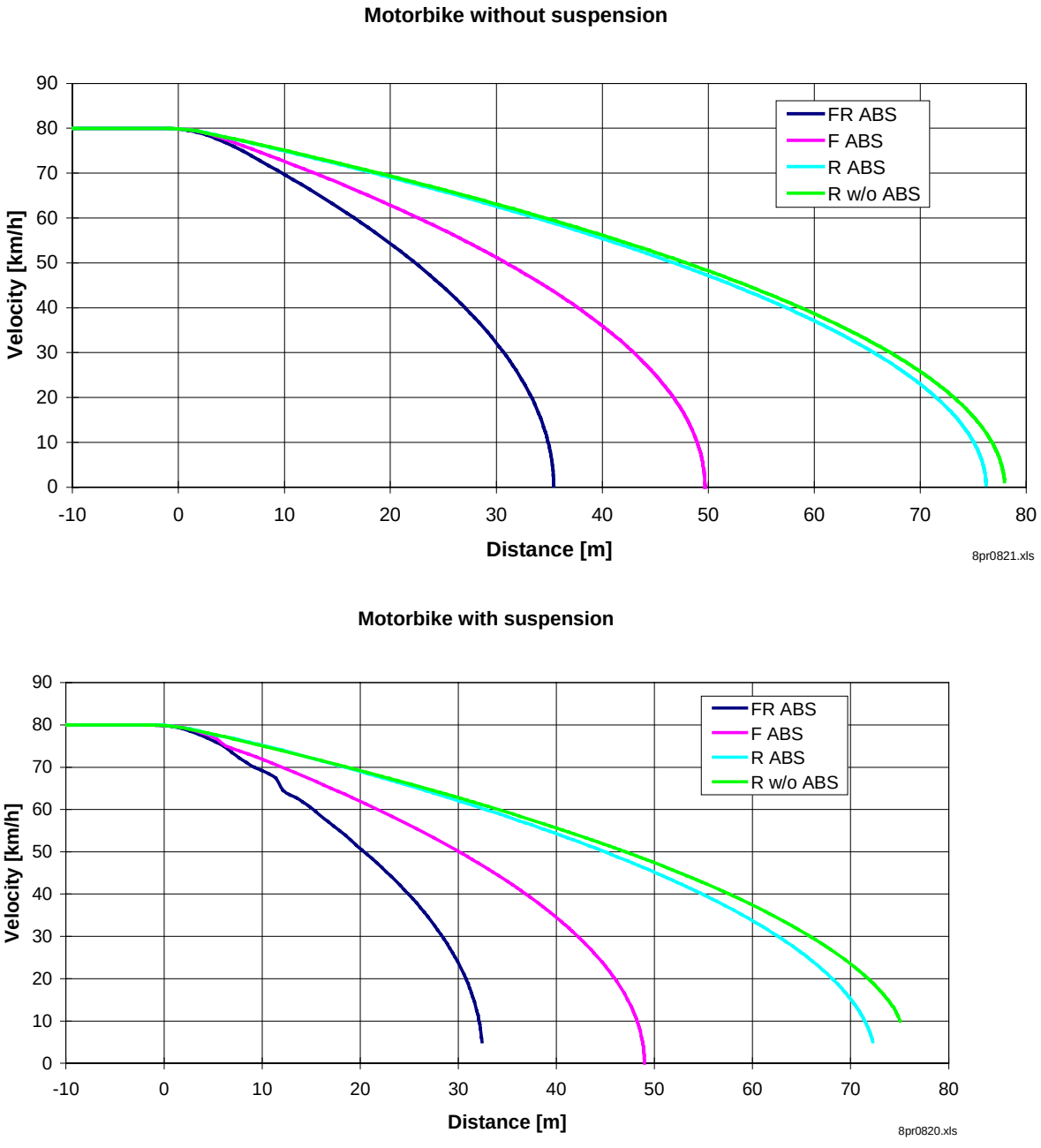

Fig. 3-4: Braking distance with and without suspension

4 Lateral dynamic

4.1 Bike control systems

To simulate open and closed loop manoeuvres, the bike velocity has to be controlled as well as the lane. Both values will be controlled by ADAMS with so-called transfer functions (TFSISO). The working concept to control, for instance, steady state cornering can be seen in the following Fig. 4-1.

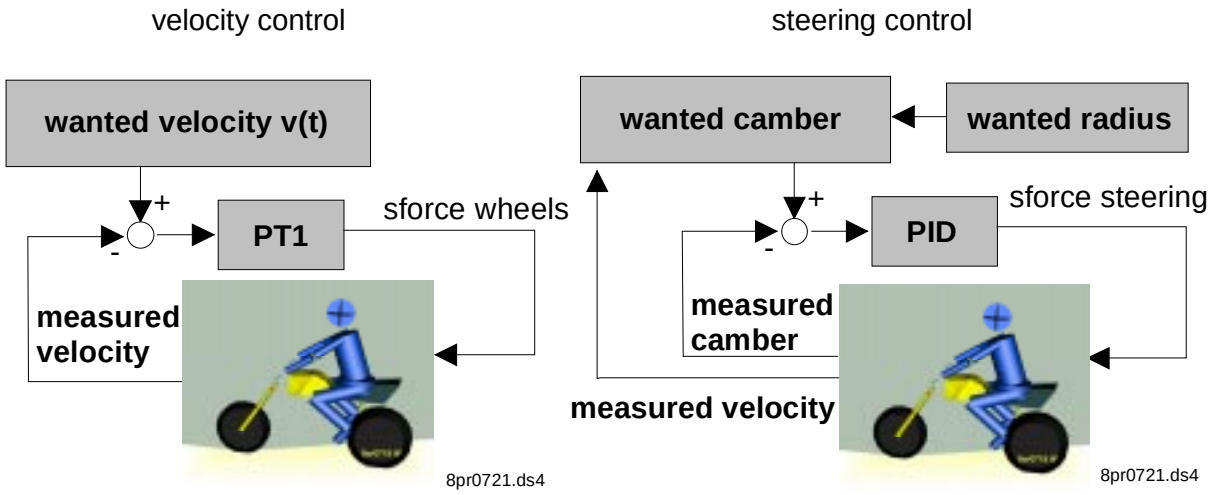

Fig. 4-1: Velocity and Steering control (steady state cornering manoeuvre)

The difference between wanted and real velocity is amplified and set to both wheels in case of braking respectively only to the rear wheel in case of acceleration. Different traction control systems can be integrated to prevent spinning wheels.

The wanted camber angle will be estimated dependent on the driving manoeuvre. In case of steady state cornering, the wanted camber angle is calculated from the actual bike velocity and the wanted circuit radius. This wanted value will be compared with the actual camber angle and controlled by a so-called PID controller. The output of this controller deliveres the force input to the steering system.

4.2 Advanced track control simulation

The simulation of lateral dynamic behaviour in combination with longitudinal dynamic will be shown on a track control system (TCS), which has been developed on the *Institut für Kraftfahrwesen Aachen*. This system is able to control the velocity and the way of an ADAMS vehicle on a given, closed way. The method of TCS will be explained on the following example.

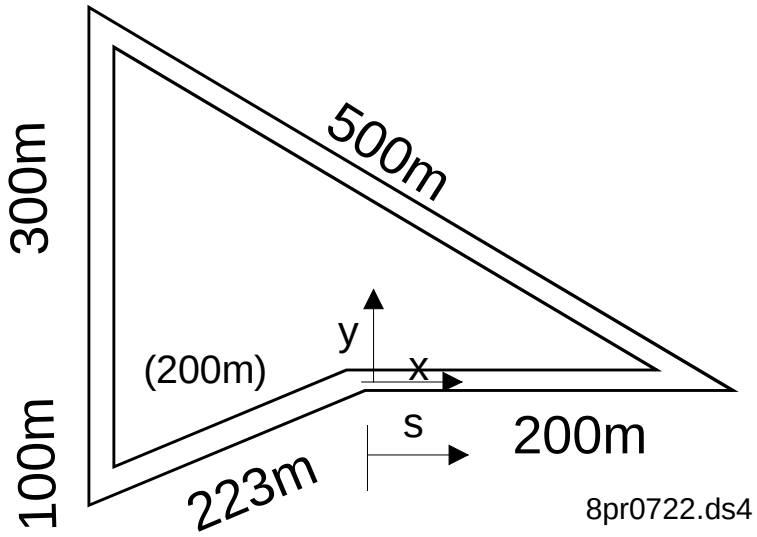

Fig. 4-1: Wanted track

Fig. 4-1 shows the lane of the wanted track. This track can be displayed as x- and y-displacement depending on the driving distance s (Fig. 4-2) which can be found by the integration of the bike velocity.

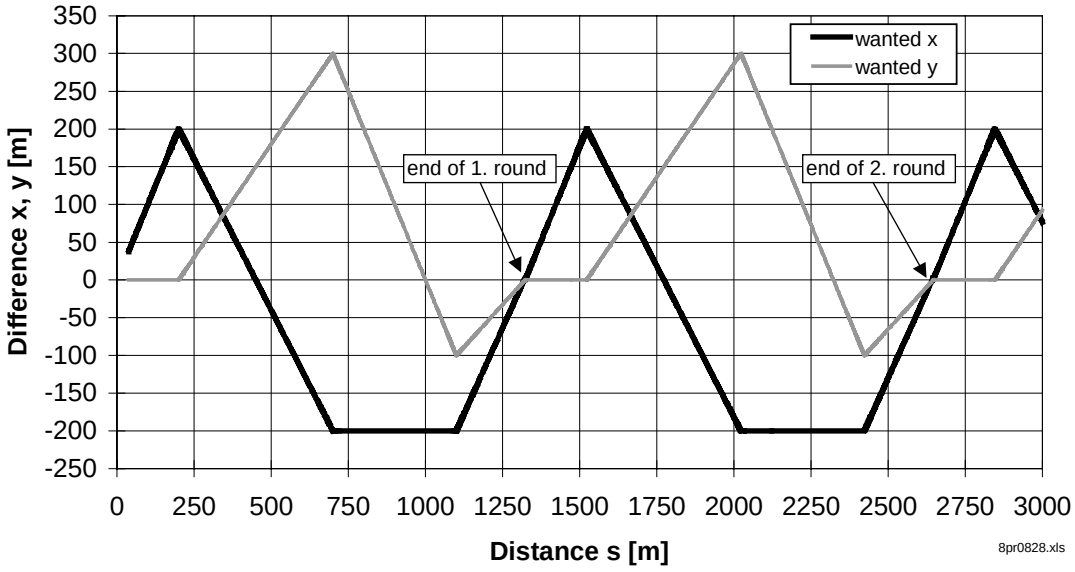

Fig. 4-2: x- and y- displacement

To react on changes in the track, two velocity depending points which look ahead are defined, one velocity control (velocity point V) and one steering control (steering point S). To prevent critical braking situations while turning, the velocity point shall be ahead the steering point.

If both points lie on the wanted lane (V1, S1 in Fig. 4-3 and Fig. 4-4), the steering angle will be set to zero, the velocity will be increased. If the velocity point is out of the wanted lane, (V2), the speed will be reduced while the steering point is on the lane. If the steering point (S3) is out of the wanted value, the wanted camber angle instruction to the steering control system (Fig. 4-1) will be given depending on the difference between wanted and real lane. The velocity is limited to a minimum so that in narrow corners the speed is nearly constant on this minimum.

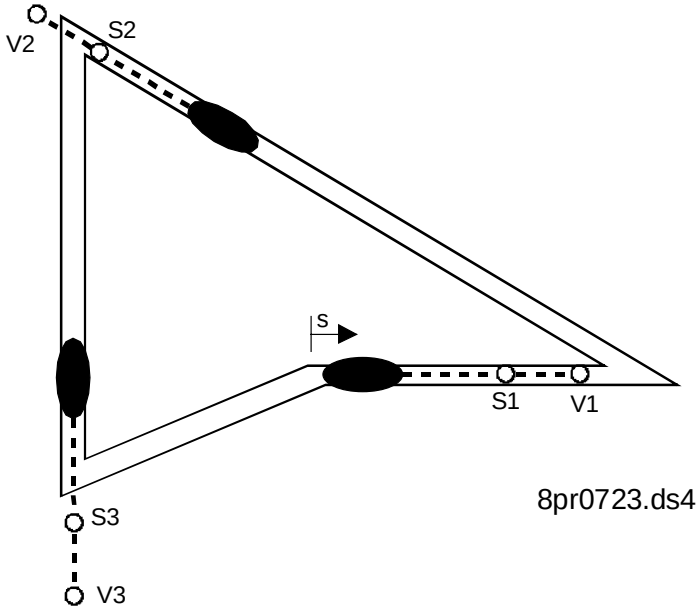

Fig. 4-3: Track control, different driving situations

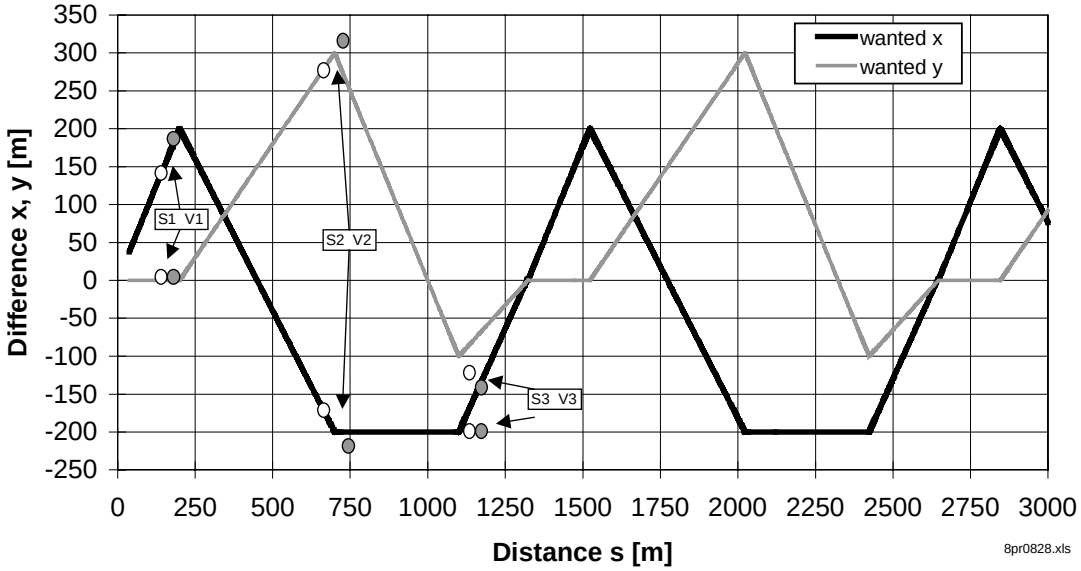

Fig. 4-4: Track control, control values

Both differences in x- and y- direction are multiplied by the sine respectively cosine of the actual rotational angle about the bike's z-axis. This has to be done to control the velocity in the actual direction of the bike and the position normal to the driving direction. Both control point distances, to the velocity point and the steering point, determines the stability of the driver model. To achieve a large stability range both points depend on the actual bike velocity.

The next Fig. 4-5 shows the wanted x- and y- displacement and the real position of the velocity point with respect to the driving distance s. Additional the wanted velocity determined by the controller and the actual bike velocity can be seen in this diagram. Depending on the difference between wanted and real position, the wanted velocity is adjusted to this deviation (input to the velocity control system in Fig. 4-1). Strait ahead, the velocity increases up to 140 km/h and decreases down to 30 km/h at narrow corners.

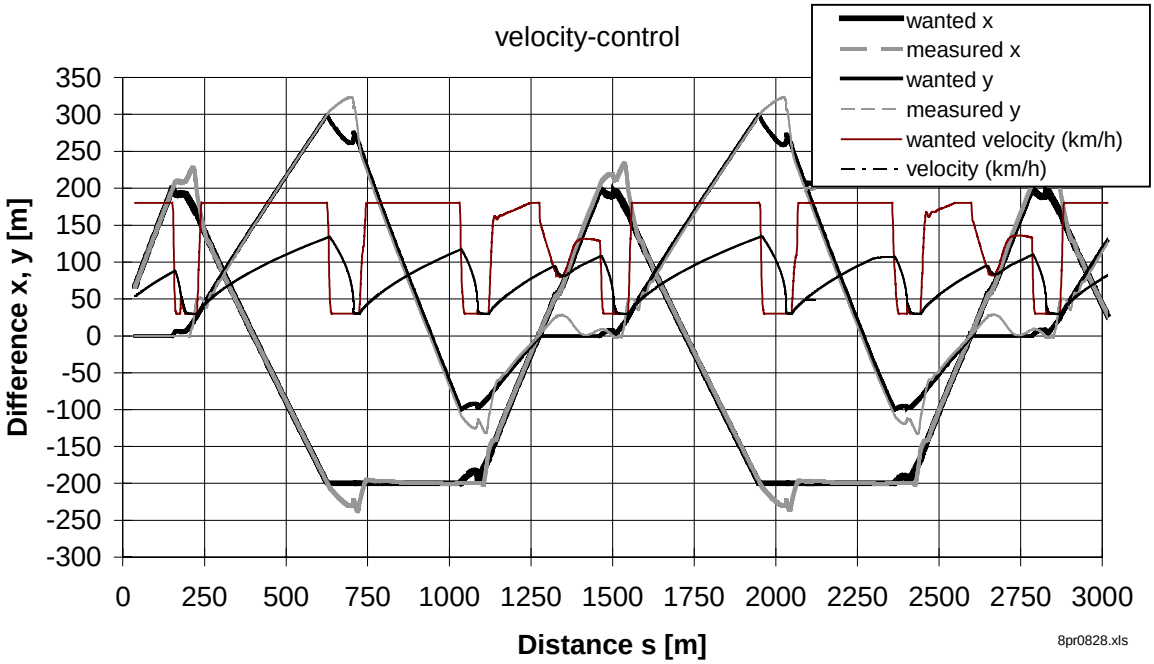

Fig. 4-5: Velocity control

The situation for the steering control system can be found in Fig. 4-6. Because of the smaller distance between the actual bike position and the steering point, the changes in the wanted x- and y- displacement are later than in Fig. 4-5. The actual velocity shows, that first of all the speed of the motorbike is reduced and afterwards the camber angle will be controlled.

The differences between wanted and real values in Fig. 4-6 (multiplied by sine and cosine of the yaw angle) will be used to calculate a wanted camber angle. The difference between wanted and real camber angle will be used as input value to the steering control system, (Fig. 4-1). Both camber angles (wanted and real one), can be seen in Fig. 4-7.

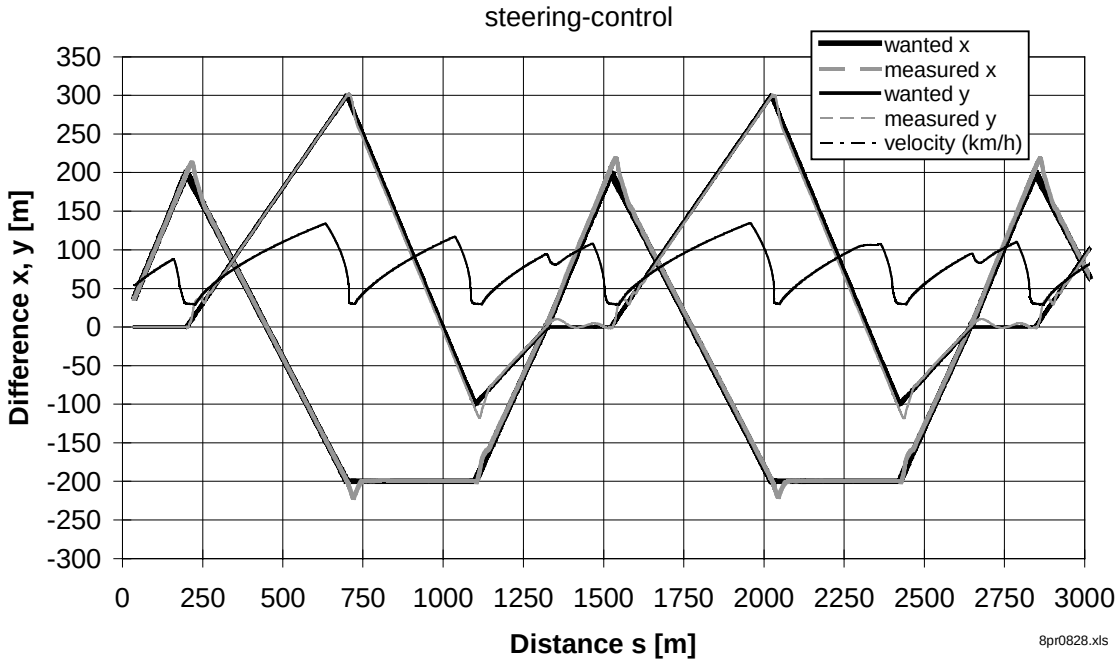

Fig. 4-6: Steering control

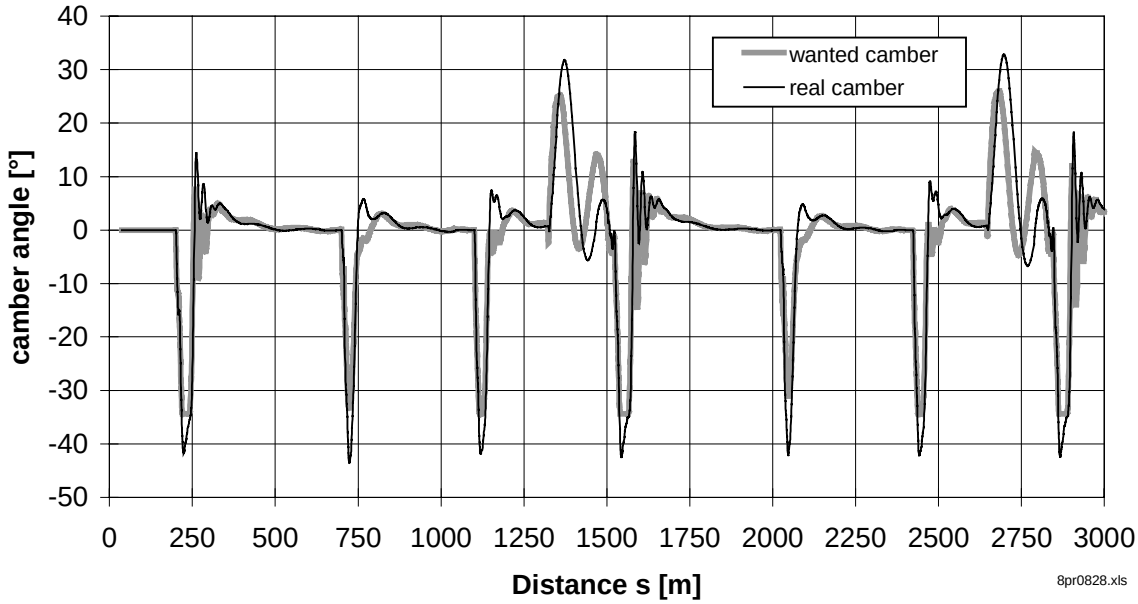

Fig. 4-7: Adjusted camber angle

The given course and the real drive line of the motorbike to this manoeuvre is shown in the next Fig. 4-8.

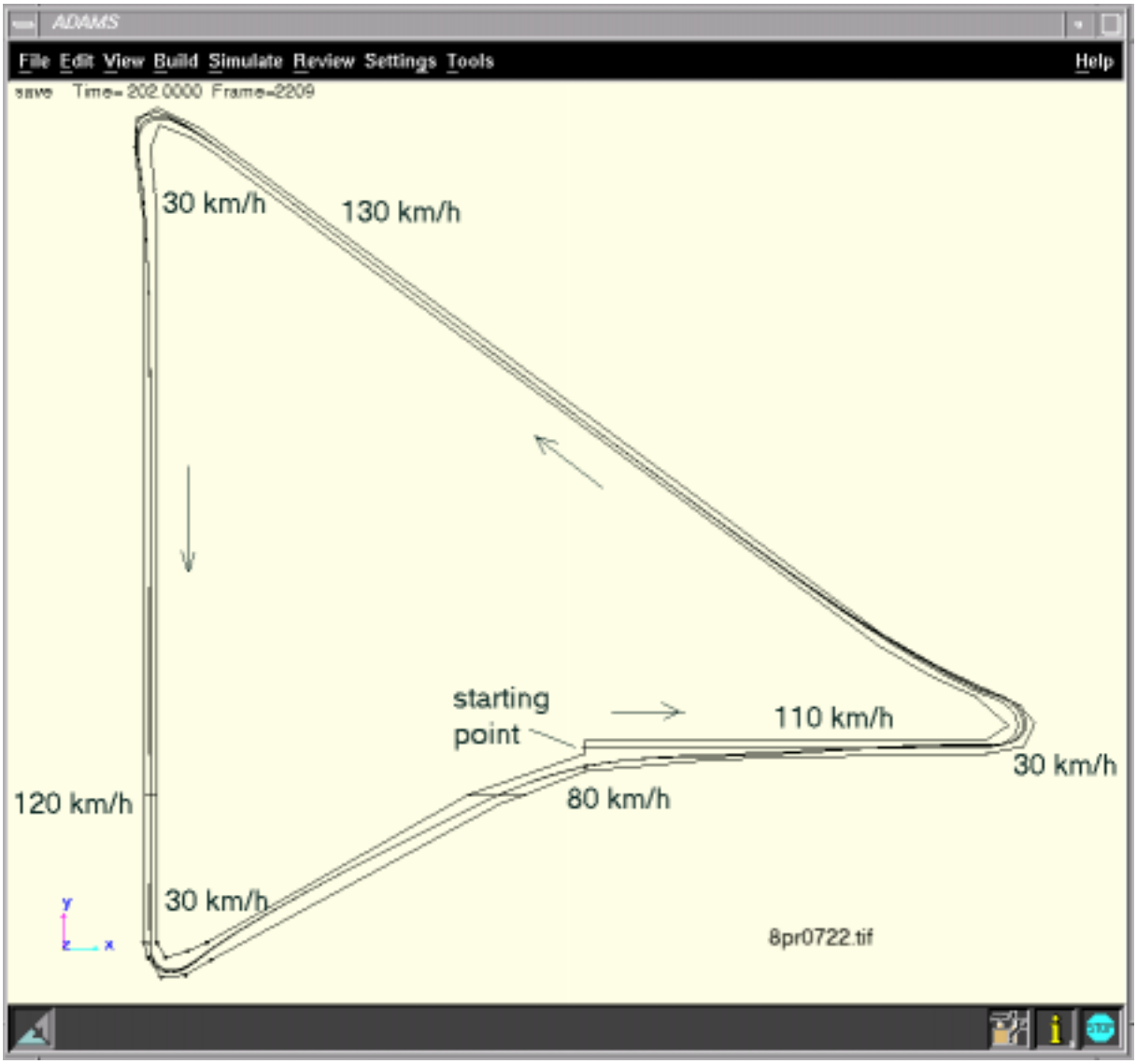

Fig. 4-8: Drive line

Because of the very hard corners in this example, the bike model is not able to do the sharp turns exactly. The used velocity control system may be improved as well as the steering control parameters. However, the track control system is able to follow the wanted lane by controlling the velocity as well as the steering angle. Additional z-displacements can be build in the track as far as lift of situations on both wheels.

5 Outlook

Dynamic Simulation Tools like ADAMS are helpful for a better understanding of multibody systems like motorbikes. Difficult equations of motion will be investigated by ADAMS, complex control systems can be added. Program integrated tyre models can be used to model non-linear tyre force characteristics in all three directions. Many applications can be

realized by these tyre models in a useful way, however, the dynamic of the ADAMS internal tyre definition seems to be improveable.

These dynamic states affect motorbike simulations more than usually passenger car simulations. Especially eigenvalue estimations cannot be done exactly at the moment with the integrated ADAMS tyre definition. Uncomfortable tyre modelling and side slip angle estimation without the ADAMS internal tyre model allows to estimate the so called wave mode eigenvalue in a good way.

Longitudinal manoeuvres can be done as well as complex combined longitudinal and lateral driving manoeuvres. The integration of control systems helps to stabilize the bike in every driving situation. The presented track control model allows to model very complex, closed loop test tracks with integrated bumps. The user written tire model takes high camber angles as well as wheel lift of into consideration.

Typical motorbike situations like stand up situations while braking and cornering or decreasing steering angle at higher lateral accelerations will be analyzed next by this model.

6 References

[BAY86] BAYER, B.
Das Pendel und Flattern von Krafträdern
Institut für Zweiradsicherheit e.V. Bochum 1986

[BRE98] BREUER, T.
Motorradsimulation im Mehrkörperdynamiksimulationsprogramm ADAMS
Studienarbeit am Institut für Kraftfahrwesen Aachen, 1998

[JAN98] JANSEN, E..
Aufbau eines Motorradmodells für Querdynamik Untersuchungen mit dem Programmpaket MATLAB
Studienarbeit am Institut für Kraftfahrwesen Aachen, 1998

[KOC80] KOCH, J
Experimentelle und analytische Untersuchungen des Motorrad-Fahrer-Systems
Fortschrittberichte VDI Reihe 12 Nr.40 VDI-Verlag 1980

[MAT96] MATLAB
Referenzmanuel zum Regelungstechnik Softwarepaket MATLAB

[SHA76] SHARP, R. S.
The dynamics of single-track vehicles
Vehicle System Dynamics Volume 5 1976 Seite 67-77

[WAL96] WALLENTOWITZ H.
Umdruck zur Vorlesung Krafträder
Forschungsgeselschaft Kraftfahrwesen Aachen mbH